INTERNATIONAL JOURNAL FOR NUMERICAL METHODS IN FLUIDS, VOL. 17, 385–400 (1993)

A NEW METHOD FOR ACCELERATING THE RATE OF CONVERGENCE OF THE SIMPLE-LIKE ALGORITHM

X. WEN AND D. B. INGHAM

Department of Applied Mathematical Studies, University of Leeds, Leeds, LS2 9JT, U.K.

SUMMARY

A pressure correction formula is proposed for the SIMPLE-like algorithm in order to improve the rate of the convergence when solving laminar Navier–Stokes equations when there is rapidly varying pressure. Based on global mass conservation, a line average pressure correction is derived by integration of the momentum equation for approximate one-dimensional flow. The use of this formula with the SIMPLE-like algorithm can rapidly build up the pressure distribution in the region where the pressure undergoes a very large change, which normally causes the rate of convergence of the SIMPLE or the SIMPLEC schemes to be slow. In order to illustrate the technique, the performances of SIMPLE and of SIMPLEC with the average pressure correction are investigated for axisymmetric flow past and through a sampler. A comparison of these two techniques shows that the average pressure correction proposed in this paper significantly accelerates the rate of convergence.

KEY WORDS SIMPLE-LIKE algorithm Average pressure correction Sampler flows

1. INTRODUCTION

Pressure correction methods have been widely used to solve Navier–Stokes equations for complex fluid flow problems ever since the pioneering work of Patankar and Spalding,[1,2] who developed the SIMPLE (Semi-Implicit Methods for Pressure Linked Equations) algorithm. Several authors have produced variants of this method in order to improve the rate of convergence of the algorithm, e.g. the SIMPLER[2] and SIMPLEC[3] methods. The mathematical development of SIMPLE-like algorithms concentrates on using the pressure–velocity relationship from linearized momentum equations. In the SIMPLE and SIMPLEC algorithms the pressure correction equations are derived from the continuity equation for each control volume, and the solution is achieved by successively predicting and correcting the velocity components and pressure. In fact, they provide a pressure correction by use of the continuity equation, which is a Poisson-type pressure correction equation. The SIMPLER algorithm starts with an estimate for the velocity field rather than for the pressure field. This change is significant, since guessing an initial condition for the velocity rather than the pressure is generally much easier. However, the pressure correction equation for SIMPLE and SIMPLEC and the pressure equation of SIMPLER are derived only at a small control volume. In the SIMPLE and SIMPLEC algorithms the pressure correction at each grid point is constrained by the local mass conservation, which can be satisfied by an incorrect local velocity. For example, if all the initial velocity components take zero values, then the local mass conservation is satisfied everywhere except at the control volumes on the boundary. Therefore, the global mass conservation is only propagated from the boundary to the whole computational domain by an iterative procedure. Because of the

0271–2091/93/170385–16$13.00
© 1993 by John Wiley & Sons, Ltd.
Received October 1992
Revised April 1993

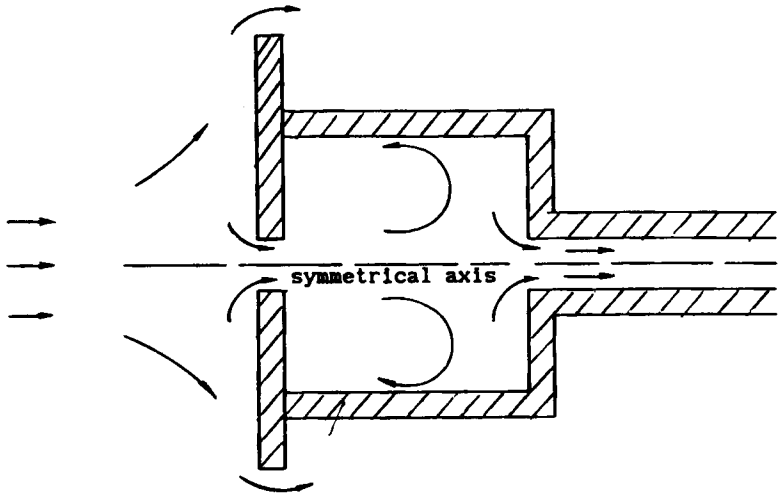

Figure 1. The sampler facing the wind

elliptic nature of the pressure correction equation, the larger the computational domain or the finer the grid used, the slower the rate of convergence. Further, in complex fluid flows the pressure correction equation is not very sensitive to large pressure drops, which results in a slow rate of convergence.

Practical and engineering problems in computational fluid dynamics inevitably involve complex geometries. For example, particle sampling has received a considerable amount of attention due to its importance in the workplace, where the concentration of airborne particles needs to be determined.[4] Samplers are usually axially symmetrical and are operated by withdrawing fluid through a small orifice in the sampler body. Figure 1 shows an example of a disk-shaped sampler. The fluid flowing past the sampler divides into two branches. One branch goes around the outside of the sampler whilst the other flows into the sampler through the orifice. When the average velocity at the sampler orifice is much larger than the free stream velocity, then the fluid which enters the sampler will be strongly contracted and undergo a very large pressure drop in the vicinity of the orifice. It then forms a cavity-like flow in the chamber of the sampler, and finally it is pumped out of the sampler through an exit pipe. At the entrance of the exit pipe the fluid undergoes another rapid pressure drop. In order to trace particle paths in the fluid flow, the detailed velocity distributions need to be obtained to a high level of accuracy. Owing to the complex nature of the flow in such circumstances, much of the previous research on this topic has been done experimentally[4] or has been based on very simple theoretical models of potential flow.[5,6] Only recently has work been done on viscous laminar[7] and turbulent flows.[8,9]

2. DISCRETIZATION AND THE SIMPLEC ALGORITHM

Chung and Ogden[10] carried out extensive experimental investigations into the aspiration coefficient of disk-shaped samplers over a wide range of operating conditions. The sampler under investigation in this paper is assumed to take the form of an axisymmetric disc with radius R and thickness d, which is followed by a cylindrical sampling chamber of radius r_1 and length l. It is assumed that the axis of the sampler is aligned with the wind, and that the fluid is aspirated through a circular central orifice on the disc with radius r_0 and pumped out through an exit pipe

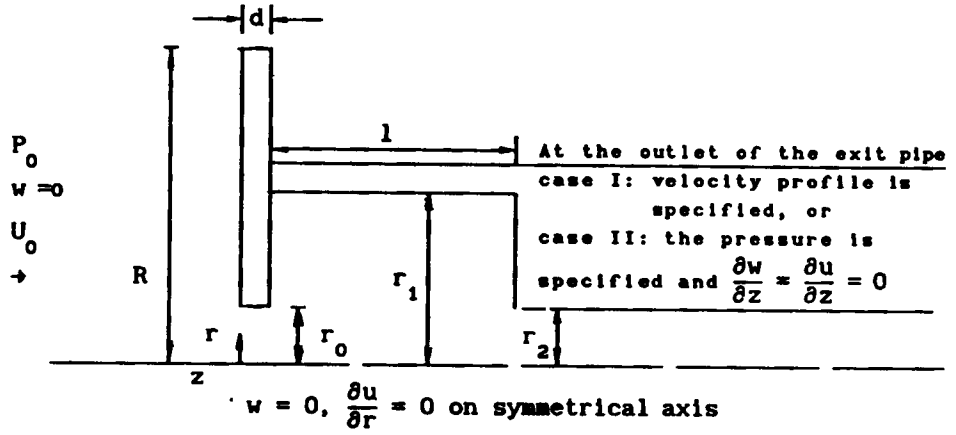

Figure 2. The mathematical model of the blunt sampler

of radius r_2 whose axis is aligned with the axis of the disc and the cylinder. Cylindrical co-ordinates are used in which r is the co-ordinate in the radial direction and z is aligned with the axis of symmetry of the sampler, as shown in Figure 2.

The continuity and momentum equations for an incompressible steady fluid flow are given, in vector notation, as

$$\nabla \cdot \mathbf{V} = 0, \tag{1}$$

$$\mathbf{V} \cdot \nabla \mathbf{V} = -\nabla p + \nabla \cdot (\nu \nabla \mathbf{V}), \tag{2}$$

where $\mathbf{V} = u\mathbf{e}_r + w\mathbf{e}_z$, $\mathbf{V}$ is the fluid velocity vector, u and w are velocity components in the radial and axial directions, respectively, $p = P/\rho$, P is the pressure, ρ is the density of the fluid and ν is the kinematic viscosity of the fluid. We now consider an arbitrary volume of fluid contained in a volume Ω which has an outer surface S and the unit outward normal to the surface is $\mathbf{n}$. We employ the Gaussian theorem, i.e.

$$\int_S \int \mathbf{n} \cdot \mathbf{V} \, dS = 0, \tag{3}$$

$$\int_S \int (\mathbf{V} \cdot \mathbf{n}) \mathbf{V} \, dS = -\int_S \int \mathbf{n} p \, dS + \int_S \int \mathbf{n} \cdot (\nu \nabla \mathbf{V}) \, dS, \tag{4}$$

in order to transform the differential forms of equations (1) and (2) into their integral forms.

The above equations have now to be solved subject to the following boundary conditions. Far upstream of the sampler there is a uniform velocity U_0, and on the sampler there is no slip and the velocity is zero. At a large radial distance from the sampler and at a large distance downstream of the sampler, derivatives of all quantities in the r and z directions, respectively, are set identically zero. On the axis of symmetry the radial velocity and the derivative of the velocity w in the r direction are zero. Further, it is assumed that the average sampling velocity at the orifice of the sampler is U_s. In the exit pipe, at the outlet of the sampler two possible types of boundary conditions may be applied: Case I where the velocity profile is specified, and Case II where the pressure is specified and the normal derivative of the two velocity components is zero.

In order to obtain accurate results, more mesh points should be employed in, and in the vicinity of, the sampler and hence non-uniform grids in both the r- and z-directions are used by means of

the following co-ordinate transformation:

$$r=f(\eta), \tag{5}$$

$$z=g(\zeta), \tag{6}$$

where η and ζ are new independent radial and axial variables and f and g are two functions which may be chosen in order to produce the required distribution of grids. In order to discretize the solution domain, a staggered grid which covers the physical domain is used. Finally the finite-difference equation for the velocity component u is obtained using equation (4) in the form

$$a_p u_p = a_E u_E + a_W u_W + a_N u_N + a_S u_S + (p_w - p_e)(h_2 h_3)_p \Delta\zeta, \tag{7}$$

where

$$a_p = a_E + a_W + a_N + a_S + \left(\frac{\nu h_1 h_3}{h_2}\right)_p \Delta\eta\,\Delta\zeta \tag{8}$$

$$a_E = \left(\frac{\nu h_2 h_3}{h_1}\right)_e \frac{\Delta\zeta}{\Delta\eta} + (h_2 h_3)_e \hat{u}_e\,\Delta\zeta, \tag{9}$$

$$a_W = \left(\frac{\nu h_2 h_3}{h_1}\right)_w \frac{\Delta\zeta}{\Delta\eta} + (h_2 h_3)_w \hat{u}_w\,\Delta\zeta, \tag{10}$$

$$a_N = \left(\frac{\nu h_1 h_2}{h_3}\right)_n \frac{\Delta\eta}{\Delta\zeta} - (h_1 h_2)_n \hat{w}_n\,\Delta\eta, \tag{11}$$

$$a_s = \left(\frac{\nu h_1 h_2}{h_3}\right)_s \frac{\Delta\eta}{\Delta\zeta} - (h_1 h_2)_s \hat{w}_s\,\Delta\eta, \tag{12}$$

and $h_1 = f'(\eta)$, $h_2 = f(\eta)$, $h_3 = g'(\zeta)$, and $\Delta\eta$ and $\Delta\zeta$ are the mesh sizes in the η and ζ directions, respectively. The quantities $\hat{u}_e$, $\hat{u}_w$, $\hat{w}_n$ and $\hat{w}_s$ are the velocities on the surfaces of the control volume and they should be replaced by schemes such as upwind, hybrid and so on. A similar expression exists for the w component of velocity.

An under-relaxation parameter E is introduced into the momentum equations and in the radial direction this may be expressed in the form

$$a_p\left(1+\frac{1}{E}\right)u_p = \sum a_{nb} u_{nb} + (p_w - p_e)(h_2 h_3)_p \Delta\zeta + \frac{a_p}{E} u_p^0. \tag{13}$$

Let p^* be the current pressure distribution and u^* and w^* be the velocities resulting from solving the radial and axial momentum equations with this pressure distribution. Therefore, we have

$$a_e u_p^* = \sum a_{nb} u_{nb}^* + (p_w - p_e)(h_2 h_3)_p \Delta\zeta + \frac{a_p}{E} u_p^0, \tag{14}$$

where $a_e = a_p(1 + 1/E)$.

If p^* is the correct pressure distribution, then the velocities u^* and w^* will satisfy the continuity equation (3). However, in general this will not be the case. We therefore introduce corrections u', w' and p' as follows:

$$u = u' + u^*, \qquad w = w' + w^*, \qquad p = p' + p^*. \tag{15}$$

The relations between the velocity and pressure corrections can be seen by substituting equa-

tions (15) into equation (14), which gives

$$(a_e-\sum a_{nb})u'_p=\sum a_{nb}(u'_{nb}-u_e)+(p'_w-p'_e)(h_2h_3)_p\,\Delta\zeta. \tag{16}$$

In the SIMPLEC algorithm, the term $\sum a_{nb}(u'_{nb}-u_e)$ is omitted and thus equation (16) becomes

$$u'_e=d_e(p'_p-p'_E), \tag{17}$$

where

$$d_e=\frac{(h_2h_3)_e\,\Delta\zeta}{a_e-\sum a_{nb}}. \tag{18}$$

The pressure correction can then be obtained by substituting all the velocity components into the continuity equation for the control volume, and this yields

$$a_pp'_p=a_Ep'_E+a_Wp'_W+a_Np'_N+a_Sp'_S+b, \tag{19}$$

where

$$b=(h_2h_3)_eu^*_e\,\Delta\zeta-(h_2h_3)_wu^*_w\,\Delta\zeta+(h_1h_2)_nw^*_n\,\Delta\eta-(h_1h_2)_sw^*_s\,\Delta\eta. \tag{20}$$

The SIMPLEC algorithm consists of the following steps:

(a) guess the velocity and pressure fields u^*, w^* and p^*;
(b) solve the momentum equations to obtain the new values of u^* and w^*;
(c) solve for the pressure correction p' and update the pressure using $p=p^*+p'$;
(d) update the velocity components u and w by using the velocity correction equations,
(e) repeat steps (b) to (d) until convergence has been reached.

The mass residual of every control volume is given by

$$R^k_{\text{mass}}=C_e-C_w+C_n-C_s, \tag{21}$$

where C_e, C_w, C_n and C_s represent the convection of mass through each face of the control volume which surrounds the point where the pressure is located. A measure of the convergence used in this paper is the sum of the mass residuals over all the control volumes, namely,

$$R_{\text{mass}}=\sum_k|R^k_{\text{mass}}|. \tag{22}$$

3. THE AVERAGE PRESSURE CORRECTION BASED ON GLOBAL MASS CONSERVATION

When the SIMPLEC algorithm was used it was found that the numerical technique did not work well on this complex fluid flow problem. The rate of convergence of the iterative scheme was extremely slow no matter what value of the relaxation factor, E, or distribution of the grids was used. Even when a very good guess as prescribed for the initial pressure and velocity fields, the rate of convergence was still extremely slow. In both Cases I and II the convergence was so slow that it would have taken many hours, or even days, of computing time on a large-scale computer in order to obtain a convergent solution. The difficulty is that it is not possible to obtain accurate velocity and pressure distributions in the vicinity of the orifice of the sampler or near the entrance to the exit pipe of the sampler. In fact the rate of convergence was much slower in the vicinity of the orifice than near the entrance to the exit pipe. This is because in the vicinity of the orifice the shape of the sampler changes very rapidly. The fluid which enters the sampler is accelerated

rapidly in order to pass through the orifice, and this is accompanied by a sharp decrease in pressure. Then, immediately after the fluid has entered the sampler chamber, there is a sudden expansion which causes the fluid to decelerate rapidly. This contrasts with the fluid motion at the entrance of the exit pipe, where the fluid simply accelerates. The pressure correction equation is not sufficiently sensitive to detect this rapid variation in the geometry of the sampler, and the iterative procedure spends many iterations building up the steep pressure gradients and large pressure drops.

The solution of the Navier–Stokes equation in the velocity–pressure formulation depends on whether we can produce the correct pressure field. For either the correct or an incorrect pressure field we can always obtain a velocity field by solving only the momentum equations, and the final correct velocity field can only be obtained if the correct pressure field has been developed. It was found that in Case I, where the velocity profile in the exit pipe is specified, divergence of the SIMPLEC technique occurs if the computational domain is extended too far into the exit pipe of the sampler, and convergence can only be obtained when the outlet boundary is very close to the entrance of the exit pipe. This is because the correct pressure field is very difficult to find if only the SIMPLEC technique is employed for the pressure correction. When the pressure in the exit pipe and upstream is specified, i.e. Case II, then we have the correct pressure upstream and in the exit pipe of the sampler at the beginning of the iteration. Thus, the iterative process has a better chance of converging than in Case I, although we found that the rate of convergence was still slow.

From the results obtained in the iterative procedures used in the SIMPLEC technique, we observed that the reason for the slow rate of convergence of the iterative procedure is that there are large differences between the fluxes of the fluid which enter through the orifice and those in the entrance to and the outlet from the exit pipe. This is due to the generation of the incorrect pressure gradient and pressure drop in the vicinity of the orifice and at the entrance to the exit pipe. Figure 3 shows the typical variation of pressure along the axis of the sampler, which illustrates the large change of pressure in the vicinities of the orifice and the entrance to the exit pipe. So an enhancement of the rate of convergence for both Case I and II is essential if this

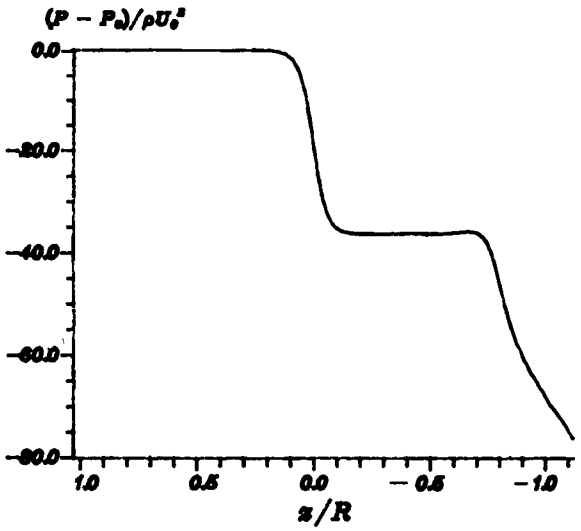

Figure 3. The pressure distribution on the axis of the sampler

method is to be used for studying blunt body sampling. In order for this problem to have a fast rate of convergence, the large pressure drop that occurs near the orifice and at the entrance to the exit pipe must be generated much faster.

It was observed that both the pressure and the velocity are dominated by changes that occur in the z-direction. Therefore, the complicated flow field may be approximately represented as a one-dimensional flow in the vicinity of the orifice and at the entrance to the exit pipe of the sampler. Then the Navier–Stokes equation (2) can be simplified to

$$\frac{1}{2}\frac{dW^2}{dz} = -\frac{d\bar{p}}{dz} + \nu\frac{d^2W}{dz^2}, \tag{23}$$

where W is the average velocity in the z-direction and $\bar{p} = \bar{p}/\rho$, where $\bar{P}$ is the average pressure. If we let W^* be the updated average velocity in the z-direction and W' be the average velocity correction, then

$$W = W^* + W'. \tag{24}$$

If the flux of fluid Q at the outlet of the exit pipe of the sampler is known,[a] then the velocity correction W' is obtained by using the global mass conservation principle, namely,

$$\int_A \rho(W^* + W')\,dS = Q, \tag{25}$$

where A is the cross-sectional area of the flow, and this yields the average velocity correction as

$$W' = \frac{Q - \int_A \rho W^*\,dS}{\int_A \rho\,dS}. \tag{26}$$

If we let $\bar{p}'$ be the average pressure correction, then the correct average pressure is given by,

$$\bar{p} = \bar{p}^* + \bar{p}', \tag{27}$$

where $\bar{p}^*$ is the updated value of the average pressure.

Inserting the values of W and $\bar{p}$ from expressions (24) and (27) into the momentum equation (23) yields

$$\frac{1}{2}\frac{dW^{*2}}{dz} + \frac{1}{2}\frac{d}{dz}(2W^*W' + W'^2) = -\frac{d\bar{p}^*}{dz} - \frac{d\bar{p}'}{dz} + \nu\frac{d^2W^*}{dz^2} + \nu\frac{d^2W'}{dz^2}. \tag{28}$$

The updated values of the velocity W^* and the pressure $\bar{p}^*$ satisfy equation (23) and hence

$$\frac{1}{2}\frac{dW^{*2}}{dz} = -\frac{d\bar{p}^*}{dz} + \nu\frac{d^2W^*}{dz^2}. \tag{29}$$

Combining equations (28) and (29) leads to

$$\frac{d}{dz}\left(W^*W' + \frac{W'^2}{2} + \bar{p}' - \nu\frac{dW'}{dz}\right) = 0, \tag{30}$$

[a] When the pressure at the outlet is specified then Q is the updated value of the flux of fluid, which is obtained through the updated velocity profile at the outlet of the sampler. When the velocity profile is specified at the outlet, then Q is given.

and hence

$$W^*W' + \frac{W'^2}{2} + \bar{p}' - \nu \frac{dW'}{dz} = C = \text{constant}. \tag{31}$$

Although the dissipation of energy in the vicinities of the orifice and the entrance of the exit pipe of the sampler is much larger than elsewhere in the solution domain, the pressure drop is a major contributor to the convection of the fluid. Therefore, locally we may neglect the effect of viscosity. Further, when the velocity correction is identically zero, then the pressure correction and the constant C should be zero. Thence, we finally obtained the average pressure correction $\bar{p}'$ caused by the average velocity correction W', namely,

$$\bar{p}' = -\left(W^*W' + \frac{W'^2}{2} \right) \tag{32}$$

The average pressure correction (32) still needs to undergo relaxation, and this correction should be added to the updated pressure p^*, so instead of using equation (32), we employ

$$p = p^* + \alpha_p \bar{p}'. \tag{33}$$

It has been found that a value of the relaxation factor α_p of about 0·5 is suitable for all the calculations performed in this paper and in all similar calculations carried out by the authors. This average pressure correction should also be used with the SIMPLE-like algorithm after each global iteration. The average pressure correction can be employed on one line or on several lines, but the value on the last line, after which the formula is not employed, should be added to all the grid nodes located downstream of this line in order to maintain the flux Q. We found that in the flow of fluid past and through samplers, the average velocity correction W' had little effect on the rate of convergence of the iterative scheme and therefore we did not use expression (24) to correct the updated velocity W^*.

4. COMPUTATIONS AND COMPARISONS

The resulting finite-difference equations of the momentum equation and pressure correction equation are solved using a line-by-line tridiagonal-matrix algorithm to solve the momentum equations with one sweep and the pressure correction equations with four sweeps. The relaxation factor was taken to have a value $E = 3$, and this produced a stable and fast rate of convergence for all the calculations presented in this paper. The treatment of the boundary conditions for the pressure correction for both Cases I and II followed the recommendations in the paper by Van and Raithby[3] (for full details of this procedure see that paper). The performance of the SIMPLEC algorithm and of the SIMPLEC algorithm implemented with the average pressure correction were made for axisymmetric, incompressible, steady-state laminar flow past a disk-shaped sampler, as shown in Figure 1. The average pressure corrections were only employed on two lines, which were located at the orifice and at the entrance of the exit pipe of the sampler: the physical flow situation with the boundary conditions non-dimensionalized with respect to the upstream velocity $|U_0|$ and the radius of the sampler R. All the comparisons made between the SIMPLEC and the SIMPLEC with the average pressure correction (32) presented in this paper were made for the Reynolds number $Re = 100$, where $Re = |U_0|R/\nu$. Further, the dimensions of the sampler were taken to be $d = 0{\cdot}02R$, $r_0 = 0{\cdot}1R$, $r_1 = 0{\cdot}74R$, $r_2 = 0{\cdot}1R$ and $l = 0{\cdot}8R$. The initial guess for the non-dimensional velocities are $u^* = 0$ and $w^* = -1$ and for the non-dimensional pressure $p^* = 0$.

Anticipating the need for a finer grid near the orifice of the sampler, we used a non-uniform grid with a 131×79 mesh to cover the solution domain by suitably choosing the transformation

functions $f(\eta)$ and $g(\zeta)$ so that a uniform grid can be employed in computational space, and the transformations were also chosen in order to produce continuous scale factors h_1, h_2 and h_3. The functions used for the calculations in this paper are

$$z=f(\eta)=0{\cdot}9/2{\cdot}07147[e^{2{\cdot}07147\eta_1}-e^{2{\cdot}07147(\eta_1-\eta)}], \quad 0<r<0{\cdot}1, \tag{34}$$

$$z=f(\eta)=(\eta-\eta_1)[-10(\eta^2+\eta\eta_1+\eta_1^2)+10{\cdot}387(\eta-\eta_1)-0{\cdot}875], \quad 0{\cdot}1<r<1{\cdot}0, \tag{35}$$

$$z=0{\cdot}15711\,e^{12{\cdot}73(\eta-\eta_2)}+0{\cdot}84289, \quad 1{\cdot}0<r, \tag{36}$$

$$g'(\zeta)=e^{5{\cdot}3115|\zeta-\zeta_1|}, \quad 0<z, \tag{37}$$

$$g'(\zeta)=1{\cdot}0, \quad -0{\cdot}8<z<0, \tag{38}$$

$$g'(\zeta)=e^{5{\cdot}3115|\zeta-\zeta_2|}, \quad z<-0{\cdot}8, \tag{39}$$

where $\eta_1=10\,\Delta\eta$, $\eta_2=50\,\Delta\eta$, $\zeta_1=80\,\Delta\zeta$, $\zeta_2=40\,\Delta\zeta$ and the grid size is $\Delta\eta=0{\cdot}01$ and $\Delta\zeta=0{\cdot}02$. This grid can cover a region in the physical space for the velocity component u with $0<r<7{\cdot}145$ and $-11{\cdot}18<z<10{\cdot}29$.

In Case I, where the velocity profile at the outlet of the exit pipe of the sampler was specified by the fully developed parabolic flow, then we have

$$w=2U_s\left[1-\left(\frac{r}{r_0}\right)^2\right]. \tag{40}$$

The strength of the sampling suction is measured by the velocity ratio U_s/U_0, and there is weak (strong) sampling if $U_s/U_0>(<)\,1$. When the boundary condition at the outlet of the exit pipe of the sampler is the specification of the velocity profile, then Figures 4 and 5 show the convergence histories of the mass residual R_{mass} and the average velocity at the orifice of the sampler, respectively, when the strength of the suction of the sampling is $U_s/U_0=0{\cdot}5$, i.e. a weak sampler,

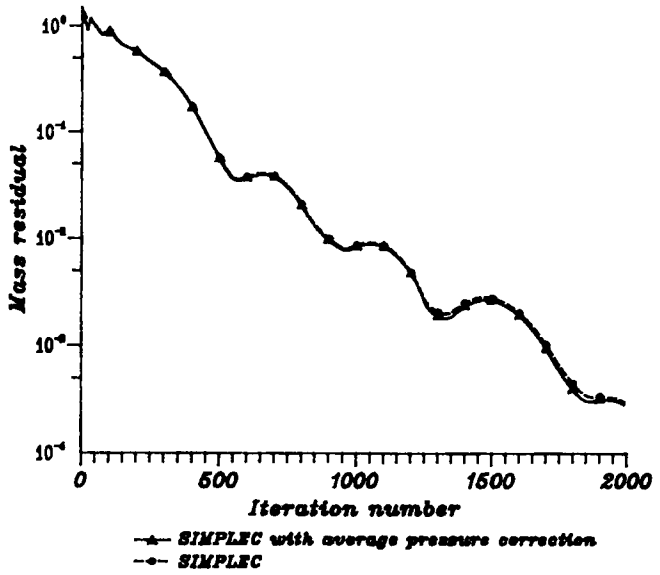

Figure 4. The convergence histories for the mass residual when $U_s/U_0=0{\cdot}5$, i.e. weak sampling

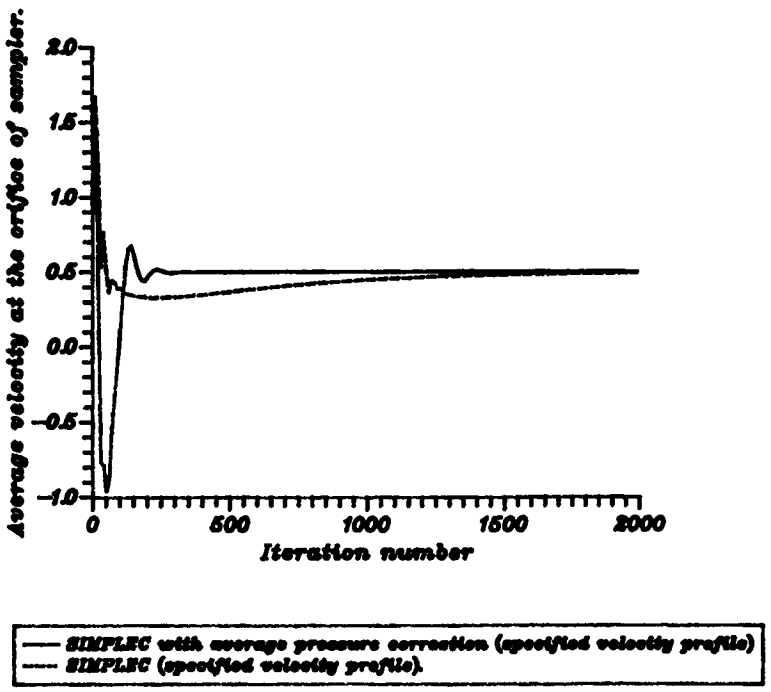

Figure 5. The convergence histories of the average velocity at the orifice when $U_s/U_0 = 0{\cdot}5$, i.e. weak sampling

when using SIMPLEC and SIMPLEC with the average pressure correction. Figure 4 demonstrates that SIMPLEC and SIMPLEC with the average pressure correction have very similar rates of convergence for the mass residual, and this is true in all the cases we have considered for weak sampling. Figure 5 shows the average velocity at the orifice of the sampler as a function of the number of iterations, and when the iterative process has converged this value should be 0·5. It is observed that after only about 400 iterations the average velocity (or the flux of fluid which enters the sampler) has reached its specified value within an error of about 10^{-5} when the average pressure correction is used, whereas this value can only be reached after about 2000 iterations when using the SIMPLEC algorithm. Therefore, the average pressure correction method has very efficiently accelerated the rate of convergence of the average velocity at the orifice (namely the sampling flux), although it has had little effect on the rate of convergence of the mass residual.

We found that as the strength of sampling increases, i.e. as the value of U_s/U_0 increases, then the rate of convergence of the SIMPLEC algorithm very noticeably slows down. Figure 6 shows the variation of the mass residual as a function of the number of iterations when $U_s/U_0 = 5{\cdot}0$, i.e. for strong sampling, when the velocity profile at the outlet is specified. It is observed from the convergence history that when the SIMPLEC algorithm is used the mass residual reduces quickly during this first 2000 iterations when the mass residual takes a value of $1{\cdot}231 \times 10^{-2}$, but after this the rate of convergence begins to slow down rapidly. In fact after 4000 iterations the mass residual is $7{\cdot}489 \times 10^{-3}$ and after 8000 iterations it has only reached a value of $3{\cdot}283 \times 10^{-3}$. When using the average pressure correction equation (32), we observe that the mass residue continues to decrease rapidly as the number of iterations increases. After 2000 iterations the mass residual reaches a value of $2{\cdot}8 \times 10^{-4}$, whilst after 4000 iterations it is $1{\cdot}055 \times 10^{-5}$. Therefore, we conclude that the rate of convergence has been remarkably improved by adopting the average pressure

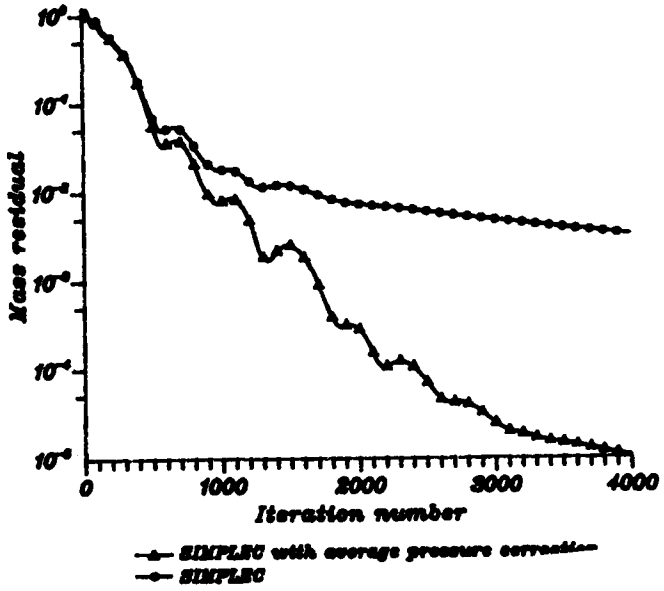

Figure 6. The convergence histories for the mass residual when $U_s/U_0 = 5{\cdot}0$, i.e. strong sampling

correction equation (32). We also found that in both cases of weak ($U_s/U_0 = 0{\cdot}5$) and strong ($U_s/U_0 = 5{\cdot}0$) sampling, almost the same rate of convergence is achieved when the average pressure correction is adopted.

Corresponding to the case of $U_s/U_0 = 5{\cdot}0$, the average velocity at the orifice of the sampler as a function of the number of iterations is shown in Figure 7. We observe that the SIMPLEC algorithm produces a very slow rate of convergence for both the average velocity at the orifice of the sampler and for the global mass conservation. After 2000 iterations the average velocity reaches a value of 2·833, in 4000 iterations it has a value of 3·668 and after 8000 iterations it only achieves a value of 4·420. Therefore, it is clear that in order to achieve its correct value, $U_s/U_0 = 5{\cdot}0$, an excessively large number of iterations will be required. However, when using the average pressure correction only 470 iterations are required for the average velocity at the orifice of the sampler, and for the sampled flux, to achieve its correct value within an accuracy of 10^{-5}. It is clear that the global mass conservation is satisfied extremely rapidly when using the average pressure correction.

The flow streamlines in the vicinity of the sampler, where the value of the stream function has been normalized with respect to $U_0 \pi R^2$, are presented in Figures 8(a) and 8(b), which correspond to the velocity fields after 4000 and 8000 iterations, respectively, as obtained when using the SIMPLEC algorithm. These flow patterns represent the velocity fields with a very low level of accuracy (see for example the dividing streamline, i.e. the line which should divide the fluid which passes into the sampler from that which passes over the sampler, which has the value of 0·05). Thus, we conclude that if only the SIMPLEC algorithm is employed, then the rate of convergence is so slow that it will take too much CPU to obtain an accurate solution.

Figures 9(a) and 9(b) present the flow patterns obtained by using the average pressure correction to implement the SIMPLEC algorithm. As observed, the result after 2000 iterations is almost indistinguishable from those obtained after 4000 iterations, and the velocity field after 2000 iterations can be used with confidence when determining the motion of the suspended solid particles.

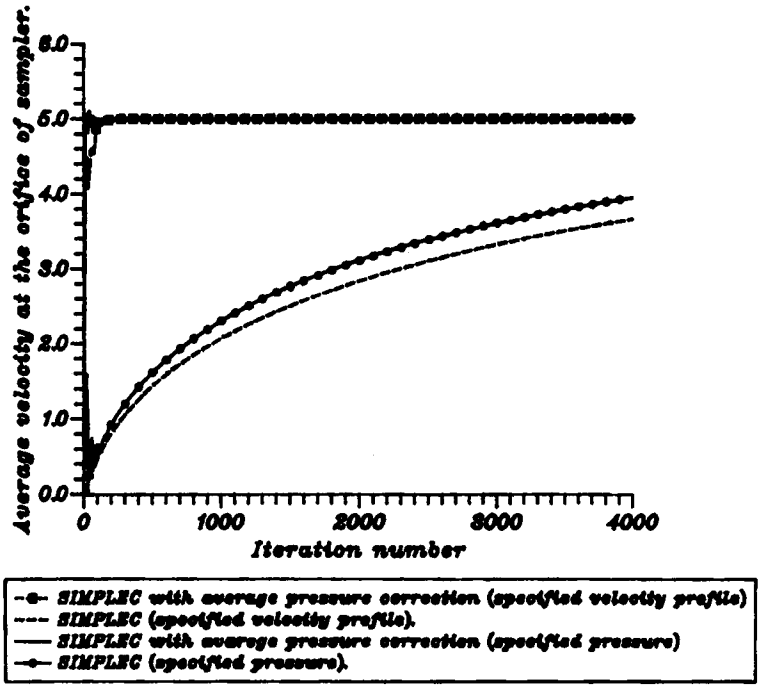

Figure 7. The convergence histories for the average velocity at the orifice when $U_s/U_0 = 5{\cdot}0$, i.e. strong sampling

Figure 10 presents the pressure distributions on the axis of the sampler as obtained by using the SIMPLEC and the SIMPLEC with the average pressure correction after 4000 iterations. The results clearly show a very steep pressure gradient and a very large pressure drop in the vicinities of the orifice and at the entrance of the exit pipe of the sampler. The pressure distribution obtained when using the SIMPLEC algorithm has a much smaller pressure drop than the correct pressure distribution. The SIMPLEC technique cannot produce a large pressure drop at the orifice of the sampler very rapidly and this has led to a loss in the flux of fluid which flows through the orifice of the sampler.

As previously observed, the local imbalance in the conservation of the mass of the fluid in each control volume is not directly equivalent to the global mass conservation. The source term in equation (20) is based on the updated velocity field, and therefore the pressure correction given by an incorrect source term cannot produce a correct pressure correction even if its exact solution for the pressure correction equation has been obtained. During the propagation of the global mass conservation from the boundary to every control volume, mass is lost in every control volume. This means that although the mass lost is small in each control volume, the total loss of mass is the sum of each of these mass loses over all of the control volumes inside the flow field. Thus, the real loss of mass will be much larger than the source term b in equation (20). Therefore, the smaller the source term the smaller the pressure correction, and this leads to an extremely slow rate of convergence when the pressure drop is very large. Obviously, the average pressure correction based on the global mass conservation directly constrains the global mass conservation on the line which is perpendicular to the direction of the fluid flow, and therefore the acceleration of the rate of convergence will be significant if the flow is dominated by the flow in one direction and the present drop is large.

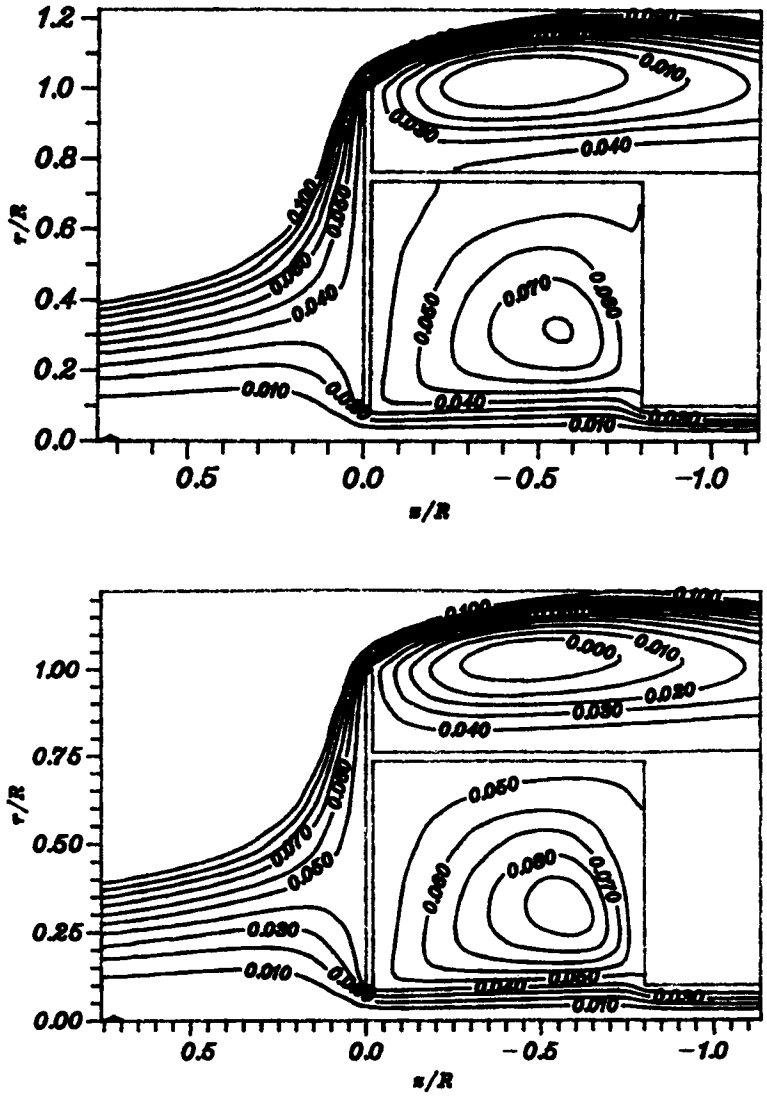

Figure 8. The flow streamlines when using the SIMPLEC algorithm: (a) after 4000 iterations; (b) after 8000 iterations

Case II, where the pressures upstream and at the outlet of the exit pipe of the sampler are specified, has also been investigated. The pressures far upstream and at the outlet of the exit pipe of the sampler were taken to be the same as those obtained from Case I when $U_s/U_0 = 5{\cdot}0$, so that the converged solution should have the same velocity field as in Case I. The results show that the convergence histories of the mass residuals are very similar (see Figure 6 for both the SIMPLEC algorithm and the SIMPLEC with the average pressure correction). The convergence histories of the average velocity at the orifice of the sampler as obtained by the SIMPLEC algorithm with the average pressure correction is only slightly different from the specification of the velocity profile near the start of the iterations in both cases. However, the rate of convergence of the average velocity produced by the SIMPLEC algorithm is different from the specification of the velocity

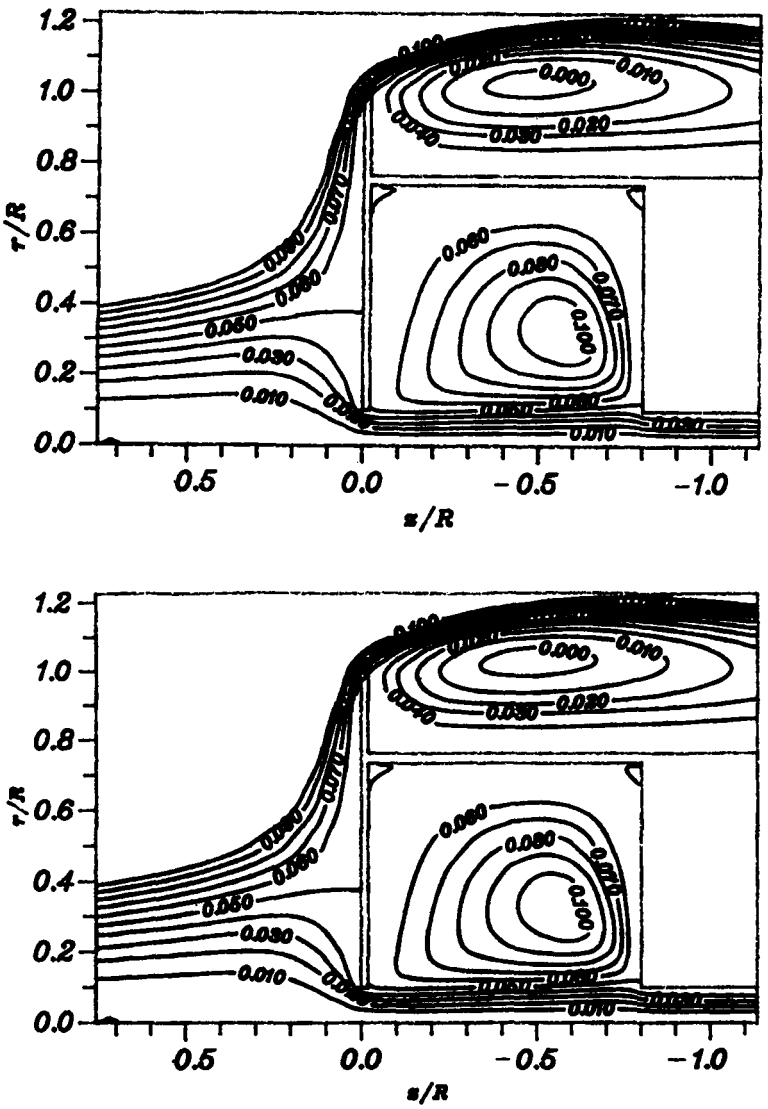

Figure 9. Flow streamlines when using the SIMPLEC algorithm with the average pressure correction: (a) after 2000 iterations; (b) after 4000 iterations

profile. When using the SIMPLEC algorithm, Figure 6 shows that when the pressure at the outlet of the sampler is specified a faster rate of convergence is obtained than when the velocity profile at the outlet of the sampler is specified. However, when the value of the average velocity is close to $U_s/U_0 = 5{\cdot}0$, the rate of convergence is still extremely slow.

Figure 11 shows the pressure distribution on the axis of the sampler after 4000 iterations when the pressure at the outlet of the exit pipe of the sampler is specified. The results show that the pressure distributions in the exit pipe of the sampler and in the vicinity of the entrance of the exit pipe are more accurate than those obtained in Case I when using the SIMPLEC algorithm. This

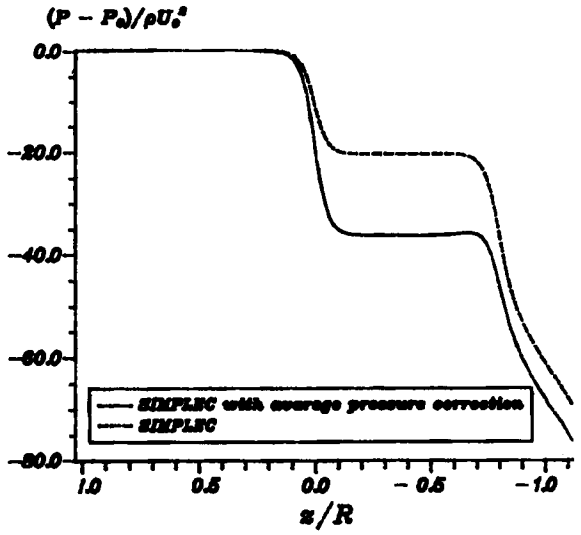

Figure 10. The pressure distributions on the axis of the sampler after 4000 iterations when the velocity profile at the outlet of the sampler is specified

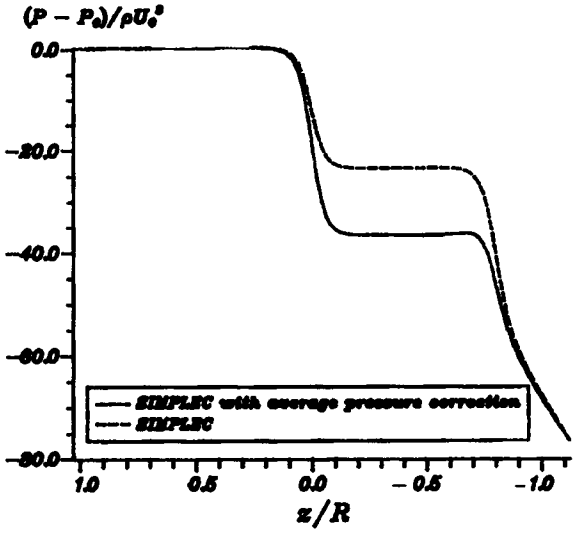

Figure 11. The pressure distribution on the axis of the sampler after 4000 iterations when the pressure at the outlet is specified

is because more accurate values of the pressure at the outlet have been specified. However, the pressure drop obtained by the SIMPLEC algorithm at the orifice is still smaller than the correct value, which is similar to Case I. The results shown in Figures 6 and 11 again indicate the fast rate of convergence when the values of the pressure far upstream and at the outlet of the exit pipe of the sampler are specified and when the average pressure correction is adopted.

5. CONCLUSIONS

The inclusion of the average pressure correction in the SIMPLEC algorithm has successfully led to a substantial enhancement in the rate of convergence of the global mass conservation, and has also produced an acceleration in the rate of convergence in the local mass residual in both cases when the velocity profile and the values of the pressures upstream and at the outlet of the sampler are specified. Therefore, a substantial reduction in the cost of obtaining numerical solutions of the Navier–Stokes equations is possible. In this paper the average pressure was applied on only two lines, which were located at the orifice and at the entrance of the exit pipe of the sampler. However, the acceleration of the rate of convergence is significant. It is clear from the example considered here that the average pressure correction equation (32) can be used to find fluid flows in more general situations when there exists a flow which is dominated by one component of the velocity, and that the rate of convergence of the method can be efficiently improved when very large pressure drops occur in the flow.

ACKNOWLEDGEMENT

The financial support of the Health and Safety Executive is gratefully acknowledged.

REFERENCES

1. S. V. Patankar and D. B. Spalding, 'A calculation procedure for heat, mass and momentum transfer in three dimensional parabolic flows', *Int. J. Heat Transfer*, **15**, 1787–1806 (1972).
2. S. V. Patankar, *Numerical Heat Transfer and Fluid Flow*, Hemisphere, Washington, DC, 1980.
3. J. P. Van and G. D. Raithby, 'Enhancements of the SIMPLE method for predicting incompressible fluid flows', *Numer. Heat Transfer*, **7**, 147–163 (1984).
4. J. H. Vincent, *Aerosol Sampling, Science and Practice*, Wiley, New York, 1989.
5. D. B. Ingham, 'The entrance of airborne particles into a blunt sampling head', *J. Aerosol Sci.*, **12**, 541–549 (1981).
6. S. J. Dunnett and D. B. Ingham, *The Mathematics of Blunt Body Sampling, Lecture Notes in Engineering*, Springer, Berlin, 1988.
7. I. P. Chung and D. Dunn-Rankin, 'Numerical simulation of two-dimensional blunt body sampling in viscous flow', *J. Aerosol Sci.*, **23**, 217–232 (1992).
8. D. B. Ingham and X. Wen, 'Dislike body sampling in a turbulent wind', 1993 (to be published in *J. Aerosol Sci.*).
9. X. Wen and D. B. Ingham, 'Blunt body sampling in a laminar and turbulent wind'. Presented at the 1992 European Aerosol Conference, Oxford, 1992, and to be published in *J. Aerosol Sci.* (1992).
10. K. Y. K. Chung and T. L. Ogden, 'Some entry efficiencies of dislike samplers facing the wind', *J. Aerosol Sci. Technol.*, **5**, 81–91 (1986).